Probabilistic Fatigue Life Modelling of Additively Manufactured Aluminum Alloys via Bayesian Inference

Zhanhua Liang[1)], Jingwen Song[2)]

1) School of Mechanical Engineering, Northwestern Polytechnical University, 710072 Xi'an, China, zhanhualiang@mail.nwpu.edu.cn

2) School of Mechanical Engineering, Northwestern Polytechnical University, 710072 Xi'an, China, jingwensong@nwpu.edu.cn

Abstract: Metal additive manufacturing (AM) of aluminum alloys has shown great potential in high-performance lightweight manufacturing industries, where the undesirable fatigue failure remains a critical challenge for reliable design. This paper focuses on probabilistic fatigue life prediction of AM aluminum alloys by considering the inherent variations in fatigue process and the uncertainties in limited fatigue data. A Bayesian inference-based uncertainty quantification framework for fatigue life prediction is proposed in this paper. Fatigue experiments are conducted with AlSi10Mg alloy specimens fabricated via Laser Powder Bed Fusion (LPBF) under two building direction (BD), generating the original experimental dataset. Four candidate models—the Coffin-Manson-Basquin, Morrow, Ostergren, and Kohout-Věchet models—are adopted for fatigue life prediction. Using the valid but scarce fatigue data, the corresponding uncertain model parameters are inferred via a sampling-based Bayesian updating technique. The results demonstrate that the 95% confidence intervals of the fatigue life models updated via Bayesian inference effectively encompass most of the experimental data.

Keywords: Additively manufactured aluminum alloys, Low-cycle fatigue, Uncertainty quantification

1. Introduction

Additive Manufacturing (AM), also known as 3D printing, offers significant advantages such as integrated forming, shortened manufacturing cycles, reduced part counts, and notable improvements in structural stiffness and weight reduction. These characteristics make it particularly suitable for the rapid manufacturing of complex structures (Zhu, 2021). Among various metal AM techniques, Laser Powder Bed Fusion (LPBF) shows considerable popularity and attracted extensive attention in the production of complex structures for aerospace applications (Blakey-Milner, 2021). A wide range of metal alloys have been successfully processed via LPBF (DebRoy, 2018). As one of the most widely used lightweight metallic materials, aluminum alloys play a significant role in weight reduction due to their excellent specific strength, good corrosion resistance, high thermal and electrical conductivity, and relatively low cost (Kotadia,2021).

Despite the considerable potential of AM aluminum alloys in the fabrication of complex geometries and rapid prototyping, it still faces numerous challenges in practical applications, particularly regarding fatigue performance (Liu, 2019). Process-induced defects such as porosity, microstructural inhomogeneity, and residual stress significantly impact the fatigue life of AM aluminum components (Sanaei,2021). Although post-processing treatments (e.g., mechanical peening and heat treatment) can partially improve performance, the additional cost and the limitations for complex structures with internal features bring new problems. Therefore, fatigue damage susceptibility has become one of the primary bottlenecks limiting the high-reliability application of aluminum alloys in additive manufacturing (Yi, 2024).

To overcome the fatigue performance limitations of additively manufactured aluminum alloys and enhance the service reliability of critical components, accurate prediction of fatigue life is essential. Numerous researchers have investigated and developed various fatigue life prediction models for additively manufactured materials. Fatigue life prediction models based on stress and strain variables have been widely adopted. For instance, Zhou et al. integrated the Basquin equation with the Goodman criterion to significantly extend fatigue life by optimizing stress distribution through adjusted scanning strategies (Zhou, 2022). Ramirez et al. employed the Basquin relationship to study the correlation between process parameters and fatigue life (Ramirez, 2024). Another widely used category of models is based on the theory of Strain Energy Density (Liao, 2023). This approach offers the advantage of comprehensively reflecting stress-strain responses and their interactions, demonstrating unique potential in characterizing fatigue damage. In response to diverse engineering requirements, SED-based fatigue theories continue to be refined, with recent studies extending to complex conditions such as different loading types and temperature ranges (Sarkar, 2017; Liao, 2021).

Although the aforementioned fatigue life prediction models can provide valuable estimates under specific conditions, an unavoidable challenge severely limits their reliability when applied to AM aluminum alloys: fatigue life data for these materials commonly exhibit significant variations, even under strictly controlled nominal test conditions (Leonetti, 2018; Zhao, 2019). Given this inherent variability, parameter calibration for traditional fatigue life models typically relies on deterministic regression analysis to establish life relationships. Such approaches suffer from two major limitations: First, they assume that data fluctuate within a narrow range around the mean—a premise that is difficult to uphold in the face of AM's significant dispersion. Second, their parameter calibration depends on large volumes of experimental data to achieve statistical significance, which poses a considerable challenge for AM research characterized by high experimental costs and limited sample sizes.

In fact, the unavoidable variations in AM materials does not stem from flaws in experimental design, but rather directly reflects the uncertainty of the additive manufacturing process itself. These uncertainties primarily stem from three sources: uncertainty in experimental measurement error, uncertainty in model parameters due to material property variability, and model form uncertainty arising from simplifications in the modeling approach.

Therefore, to effectively characterize the fatigue behavior of AM aluminum alloys under uncertain conditions and establish reliable predictive models, it is imperative to move beyond deterministic mean-value analyses. The theory of Uncertainty Quantification (UQ) provides a powerful framework to address this challenge. UQ aims to explicitly characterize, propagate, and quantify the multiple sources of uncertainty mentioned above. It is particularly adept at constructing probabilistic predictive models using limited experimental data, thereby enabling more robust estimation of fatigue life and its confidence interval. Within the UQ framework, experimental error uncertainty and model parameter uncertainty can be quantitatively assessed through Bayesian updating theory. This approach incorporates prior knowledge and experimental data to probabilistically correct and update model parameters (Beck, 1998), effectively quantifying the effects of material variability and experimental errors on model predictions (Bi, 2023). Several researchers have applied Bayesian updating theory to fatigue life prediction of additively manufactured materials. For instance, Wang et al. proposed a reliability framework integrated with uncertainty quantification to predict the low-cycle fatigue (LCF) life of turbine disks (Wang, 2017). He et al. developed an efficient Bayesian neural network model for uncertainty quantification in multiaxial fatigue life prediction (He, 2024). These studies demonstrate that Bayesian updating, as a key tool within UQ, provides essential methodological support for achieving highly reliable fatigue life predictions of AM aluminum alloys and other materials in uncertain environments.

The present research focuses on incorporating the abovementioned model parameter uncertainties and model form uncertainties into fatigue life prediction models of AM aluminum alloys. For selected candidate fatigue life models, the Bayesian updating methodology is applied to calibrate model parameters using limited fatigue data. This approach can provide point estimates (e.g., posterior mean) of the parameters but also quantifies their posterior uncertainty. The parameter uncertainties are subsequently propagated to obtain the probability distribution of the predicted fatigue life. Furthermore, through comparative analysis of model predictions under different building direction, the influence of building direction on the fatigue performance of the additively manufactured aluminum alloy is systematically revealed.

2. AM specimens of aluminum alloys and experiments

The material used in this research was AlSi10Mg alloy, with spherical powder employed for the LPBF fabrication process. The main chemical composition and particle size distribution are presented in Table I.

Table I. The main chemical composition and particle size distribution

Composition (wt%)	Al Bal.	Si 9.0-11.0	Mg 0.20-0.45	Fe ≤0.50	Cu ≤0.03	Zn ≤0.10	Ti ≤0.15	Mn ≤0.40
Particle size distribution (%)	D10 μm 15-30	/ /	D50 μm 30-50	/ /	/ /	D90μm 55-75	/ /	/ /

The LPBF process was conducted on a BLT-S400 metal additive manufacturing system using optimized parameters provided by the manufacturer. Key process parameters included a laser spot size of 80 μm, a laser power of 500 W, and a powder layer thickness of 30 μm. To enhance densification, particular attention was paid to the rotation of the scanning direction between successive layers. Owing to the continuous rotation of the scan direction across layers, the material can be considered transversely isotropic relative to the building direction (i.e., the direction of layer-by-layer material deposition in laser powder bed fusion). A series of specimens were fabricated for microstructural and mechanical characterization. All specimens underwent heat treatment after the LPBF process to improve their mechanical properties.

For the cyclic tension-compression tests, two sets of $\phi 13\,\mathrm{mm} \times 110\,\mathrm{mm}$ cylindrical bars were printed. One set was printed parallel to the building direction, and the other perpendicular to it. Each set consisted of ten cylindrical rods, which were subsequently machined into standardized specimens for cyclic testing. The strain-controlled cyclic tension-compression tests were conducted on an MTS servo-hydraulic testing system in compliance with the standard specifications of GB/T 15248-2008. A strain ratio $R_{\varepsilon} = -1$ and a loading frequency $f = 0.1\,\mathrm{Hz}$ were applied. Throughout the tests, the longitudinal strain was measured and controlled using an MTS extensometer with a 12 mm gauge length.

The building direction and geometry of the specimens used in the cyclic tests are illustrated in Figure 1. global coordinate system was established to facilitate specimen identification, with the x-axis parallel to the building direction and the y–z plane perpendicular to it. All specimens were labeled according to their building direction. For instance, specimens subjected to cyclic tension-compression parallel to the building direction are designated as S followed by the specimen number, while those loaded perpendicular to the building direction are labeled H followed by the specimen number.

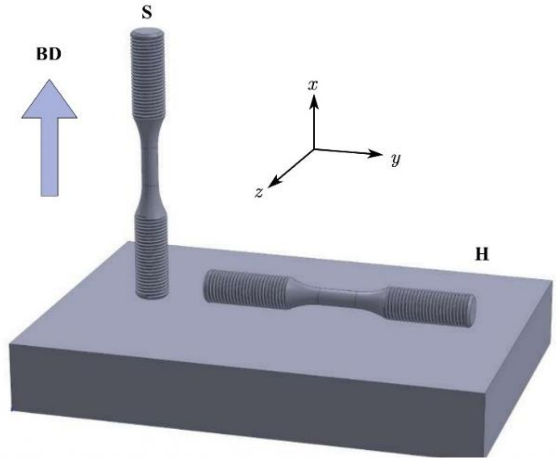

Figure 1. Specimens for cyclic tension-compression experiments.

The strain-fatigue life data for the two building direction are presented in Figure 2, along with their corresponding fitted strain-life curves. Based on the fitted curves, when the strain amplitude exceeds 0.4, specimens subjected to cyclic loading perpendicular to the building direction exhibit higher fatigue lives than those loaded parallel to the building direction. Conversely, at strain amplitudes below 0.4, specimens loaded parallel to the building direction demonstrate relatively longer fatigue lives.

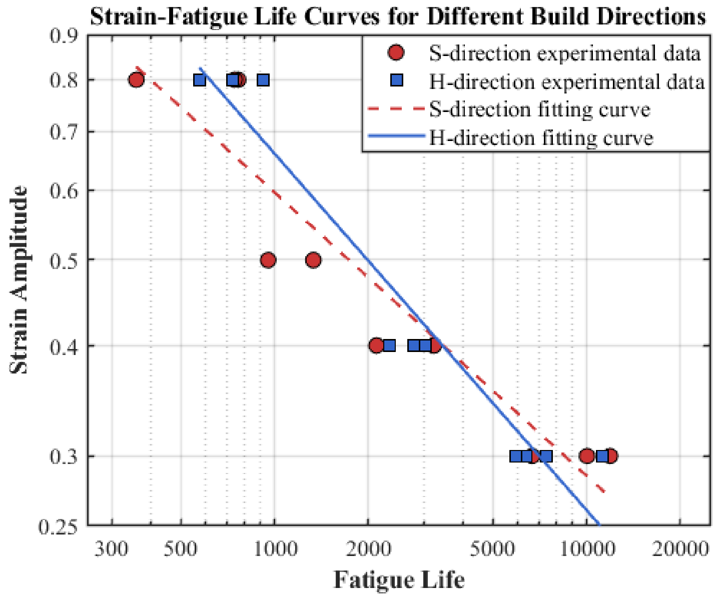

Figure 2. Strain–Fatigue Life Behavior under Different Building direction.

3. Bayesian inference of candidate Fatigue Life Model Parameters

3.1. BAYESIAN UPDATING THEORY

The Bayesian updating process is based on the well-known Bayes' theorem, which is generally expressed as:

$$P(\boldsymbol{\theta} \mid \boldsymbol{Y}_{\text{obs}}) = \frac{L(\boldsymbol{\theta} \mid \boldsymbol{Y}_{\text{obs}}) P(\boldsymbol{\theta})}{\int L(\boldsymbol{\theta} \mid \boldsymbol{Y}_{\text{obs}}) P(\boldsymbol{\theta}) d\boldsymbol{\theta}}, \tag{1}$$

where $\boldsymbol{\theta}$ represents the variables to be updated (e.g., model parameters), and $\boldsymbol{Y}_{\text{obs}}$ denotes the observed data of model responses. The term $P(\boldsymbol{\theta}|\boldsymbol{Y}_{\text{obs}})$ is the posterior probability density function (PDF) of the variables conditional on the observations; $L(\boldsymbol{\theta}|\boldsymbol{Y}_{\text{obs}}) = P(\boldsymbol{Y}_{\text{obs}}|\boldsymbol{\theta})$ is the likelihood function, indicating the probability of observing the data $\boldsymbol{Y}_{\text{obs}}$ given the variables $\boldsymbol{\theta}$; and $P(\boldsymbol{\theta})$ is the prior PDF, representing pre-existing knowledge about the variables before updating. The multidimensional integral $c_E = \int L(\boldsymbol{\theta}|\boldsymbol{Y}_{\text{obs}}) P(\boldsymbol{\theta}) \mathrm{d}\boldsymbol{\theta}$, known as the model evidence, serves as a normalization constant ensuring that the posterior PDF integrates to unity.

The posterior PDF quantifies the joint probability distribution of the parameters by inference from the observed data. This indicates that the objective of Bayesian updating is not to determine specific parameter values corresponding to individual observations, but rather to infer the overall probability distribution of the parameters. A key advantage of this approach lies in its ability to integrate prior knowledge with observed data, thereby yielding more accurate estimates of unknown variables while quantifying the uncertainty associated with these estimates.

Within the Bayesian framework, initial knowledge regarding unknown adjustable parameters—such as information derived from prior studies or expert judgment—is represented through the prior PDF. When the upper and lower bounds of a parameter are known, a uniform distribution is often adopted as a suitable prior. Conversely, if the mean value and relative error of a parameter are available, a Gaussian distribution may serve as an appropriate prior.

The likelihood function provides a measure of the discrepancy between the available experimental data $\boldsymbol{Y}_{\text{obs}}$ and the corresponding model predictions $\boldsymbol{Y}_{\text{pre}}$. In this study, this discrepancy is conventionally modeled as a Gaussian distribution with zero mean and a covariance matrix Σ. Under the assumption that the observations are mutually independent, the covariance matrix Σ reduces to a diagonal matrix. Correspondingly, the likelihood function is expressed as:

$$L(\boldsymbol{\theta} \mid \boldsymbol{Y}_{\text{obs}}) = (2\pi)^{-n/2} \mid \Sigma \mid^{-1/2} \exp\left(-\frac{1}{2} \left(\boldsymbol{Y}_{\text{obs}} - \boldsymbol{Y}_{\text{pre}} \right)^{\mathrm{T}} \Sigma^{-1} \left(\boldsymbol{Y}_{\text{obs}} - \boldsymbol{Y}_{\text{pre}} \right) \right) \tag{2}$$

where $\boldsymbol{\theta}$ denotes the parameters to be updated, and n denotes the dimension of the observed data $\boldsymbol{Y}_{\text{obs}}$.

Special attention must be paid to the definition of the likelihood function. Different choices of likelihood functions can lead to substantially different accuracy and efficiency in the updating procedure; therefore, the selection should be made carefully. The use of an inappropriate likelihood function may result in posterior distributions that deviate significantly from the prior, failing to incorporate meaningful information from the data.

The principles of Bayesian updating provide a rigorous theoretical framework for the uncertainty quantification of model parameters. To efficiently implement this Bayesian inference process in practical applications, this chapter employs two computational methods: the Bayesian Updating with Structural reliability methods (BUS) and the Particle Filter (PF) method. The BUS method reformulates the Bayesian updating problem as a structural reliability problem, leveraging well-established and efficient algorithms from that field. The PF method, on the other hand, is a sequential Monte Carlo sampling technique particularly suited for parameter estimation problems. It is worth noting that Bayesian updating techniques continue to evolve, with emerging advanced methods offering alternatives for complex updating scenarios. For instance, sampling-based adaptive Bayesian quadrature provides novel solutions for model updating, serving as a reference for methodologies beyond the scope of this study (Song, 2025).

3.2. Bayesian Updating of Model Parameters

3.2.1. *Inference for Coffin–Manson–Basquin Model Parameters*

The Coffin–Manson–Basquin model represents a landmark theory in fatigue life prediction, founded through seminal contributions by Basquin , Coffin and Manson, and later integrated into a unified framework. Basquin first established the power-law relationship between stress and life in high-cycle fatigue, revealing failure mechanisms dominated by cyclic elastic deformation (OH, 1910). Independently, Manson and Coffin proposed a plastic strain–life equation for low-cycle fatigue, highlighting the critical role of cumulative plastic damage (Manson, 1953; Coffin, 1954). The integration of these approaches resulted in a total strain–life model that unified fatigue life prediction from short to long lifetimes. The mathematical expression of the model is given as follows:

$$\varepsilon_a = \frac{\sigma_f'}{E}\left(2N_f\right)^b + \varepsilon_f'\left(2N_f\right)^c \tag{3}$$

where ε_a denotes the stress amplitude, σ_f' denotes the fatigue strength coefficient, E denotes the Young's modulus, b denotes the fatigue strength exponent, ε_f' denotes the fatigue ductility coefficient, and c denotes the fatigue ductility exponent.

The fatigue strength coefficient σ_f', fatigue strength exponent b, fatigue ductility coefficient ε_f', and fatigue ductility exponent c were treated as the model parameters to be updated. Figure 3 displays the PDF curves of the updated model parameters. As can be observed, there is no significant difference between the marginal posterior PDF obtained using the BUS and PF methods. Compared to the uniform prior distributions, the fatigue ductility coefficient ε_f' and the fatigue ductility exponent c exhibit noticeable updating effects, whereas the updates for the fatigue strength coefficient σ_f' is less pronounced. This discrepancy arises because σ_f' and b primarily govern the elastic strain component in the model, while ε_f' and c control the plastic strain component. In low-cycle fatigue of aluminum alloys, the behavior is dominated more significantly by plastic strain than by elastic strain. Consequently, the parameters controlling elastic strain (σ_f' and b) cannot be effectively updated using only low-cycle fatigue data.

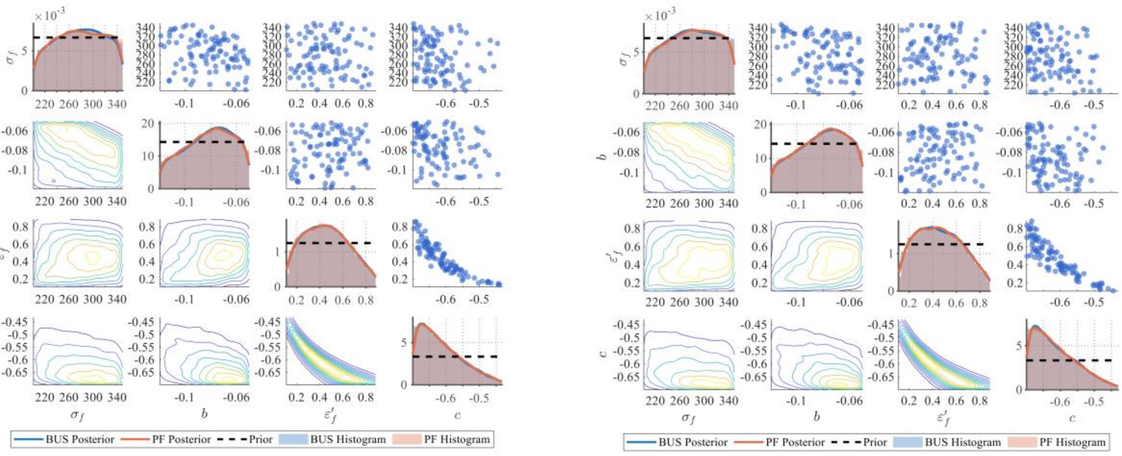

(a) (b)

Figure 3. Posterior PDF and Posterior Samples for the Coffin–Manson–Basquin Model: (a)Posterior PDF and Posterior Samples in the S direction; (b)Posterior PDF and Posterior Samples in the H direction

The lower triangular section of the figure shows contour plots of the joint posterior PDF for pairs of parameters, enabling analysis of correlations between them. It can be observed that the updated parameters ε_f' and c exhibit a clear correlation. The upper triangular section presents scatter plots of samples drawn from the joint posterior PDF, illustrating the spatial distribution of the parameter samples.

3.2.2. *Inference for Morrow Model Parameters*

The energy-based approach is an well-established method for predicting fatigue life. Morrow proposed that fatigue damage can be considered as a continuous and irreversible process of strain energy accumulation (Morrow, 1965).Theoretically, the plastic strain energy absorbed in a complete cycle can be obtained by integrating the area enclosed by the hysteresis loop, denoted as ΔW_p. The relationship between the plastic strain energy density ΔW_p and the fatigue life N_f is expressed as follows:

$$\Delta W_p N_f^{\beta} = C_1 \tag{4}$$

where both β and C_1 are material constants.

The plastic strain energy density ΔW_p was determined by calculations of the area of hysteresis loop at the half-life cycle of each specimen during testing. The material constants β and C_1 were updated using both the BUS and PF methods. Note that the prior distributions of the parameters to be updated were appropriately adjusted and are not identical for the two building directions. The posterior results obtained from the PF and BUS methods show good agreement. Furthermore, the posterior means of both β and C_1 in the H direction were higher than those in the S direction.

Figure 4 shows the PDF curves of the updated model parameters. It can be observed that the marginal posterior PDF obtained by the BUS and PF methods show no significant differences. The parameter updating effects are notable for both building direction.

The lower triangular section displays contour plots of the joint posterior PDF for parameter pairs, allowing analysis of correlations between parameters. The figure indicates a clear correlation between the updated parameters β and C_1. The upper triangular section presents scatter plots of samples drawn from the joint posterior PDF, illustrating the spatial distribution of the samples.

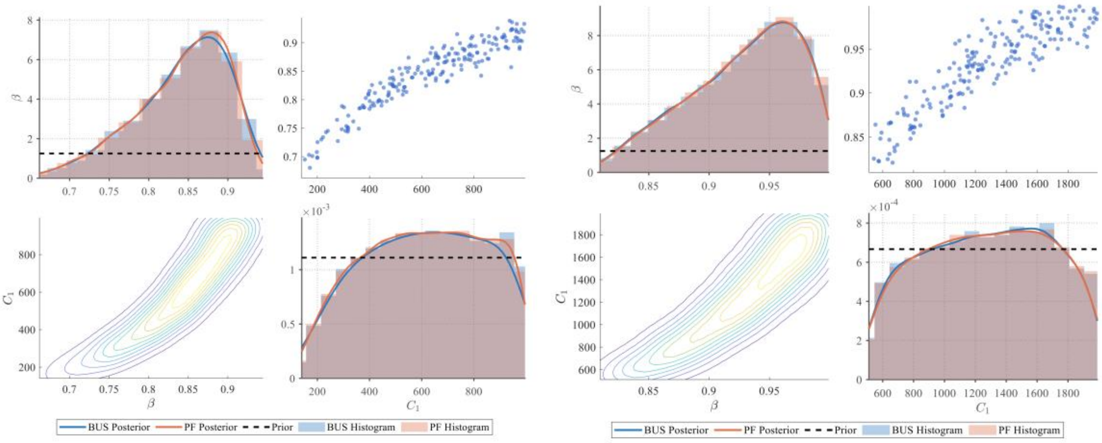

(a) (b)

Figure 4. Posterior PDF and Posterior Samples for the Morrow Model: (a) Posterior PDF and Posterior Samples in the S direction; (b) Posterior PDF and Posterior Samples in the H direction.

3.2.3. *Inference for Ostergren Model Parameters*

Ostergren proposed a strain energy damage function model analogous to the material toughness equation (Ostergren, 1976). The strain energy damage function, denoted as ΔW_s, is approximated by the product of the inelastic strain range $\Delta\varepsilon_{in}$ and the maximum tensile stress $\sigma_{\max}$:

$$\Delta W_s = \Delta\varepsilon_{in}\sigma_{\max} \tag{5}$$

where the inelastic strain range $\Delta\varepsilon_{in}$ can be substituted by the plastic strain range $\Delta\varepsilon_p$ under pure fatigue conditions. The relationship between the strain energy damage function and fatigue life N_f can be expressed as:

$$\Delta W_s N_f^m = C_2 \tag{6}$$

The maximum tensile stress $\sigma_{\max}$ was obtained directly from experimental data, and the plastic strain range $\Delta\varepsilon_p$ was derived from processed experimental data, allowing the calculation of the strain energy damage function ΔW_s for each specimen. Using the observed data of ΔW_s, the material constants m and C_2 were updated.

The PDF curves of the updated model parameters are shown in Figure 5. It can be observed that the marginal PDFs shows good consistencies between BUS and PF methods. The parameter updating effects are notable for both building direction.

The lower triangular section of the figure displays contour plots of the joint posterior PDF for parameter pairs, allowing analysis of correlations between the parameters. The upper triangular section presents scatter plots of samples drawn from the joint posterior PDF, illustrating the dependencies of spatial distribution among the samples. It indicates that the two model parameters m and C_2 has significant positive correlation effects, where the case of H direction shows a stronger linear correlation than that of S direction. The correlations would inevitably influence the accuracies of subsequent fatigue life predictions.

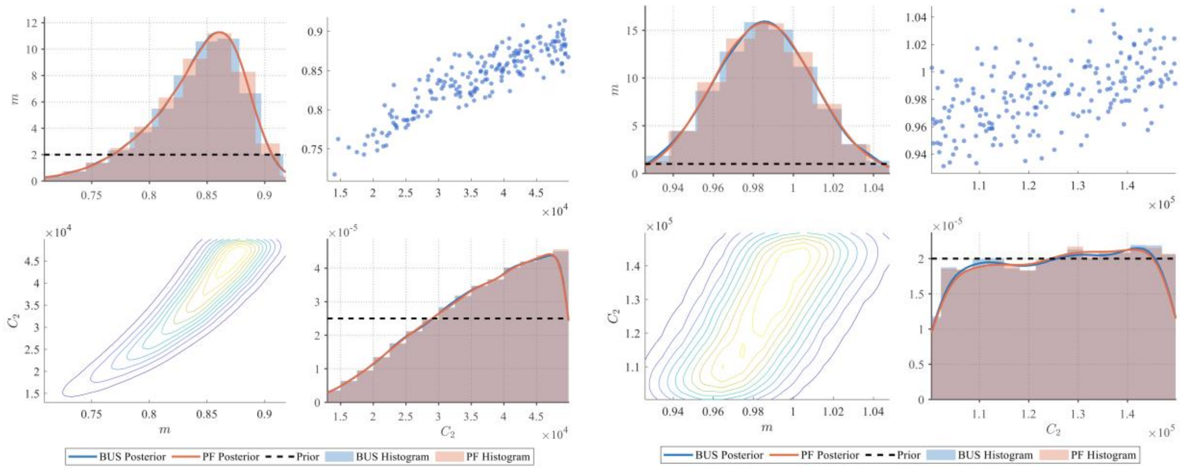

Figure 5. Posterior PDF and Posterior Samples for the Ostergren Model: (a) Posterior PDF and Posterior Samples in the S direction; (b) Posterior PDF and Posterior Samples in the H direction.

3.2.4. *Inference for Kohout-Věchet (K-V) Model Parameters*

Kohout and Věchet proposed a fatigue life model based on a stress-based damage parameter (Kohout, 2001). This model describes fatigue life behavior by adjusting the geometry of the S–N curve, namely its slope and position. This model enables prediction of the fatigue life of metallic materials in both the low-cycle fatigue (LCF) and high-cycle fatigue (HCF) regimes, as given in Equation (8):

$$\sigma_{max} = \sigma_{\mathrm{UTS}} \left(\frac{1 + \frac{N_f}{B}}{1 + \frac{N_f}{C}} \right)^b \tag{7}$$

where $\sigma_{\max}$ denotes the maximum tensile stress, σ_{UTS} denotes the ultimate tensile strength, and B, C, and b are material constants. Here, B represents the number of cycles at the intersection of the finite-life region tangent and the asymptote at the ultimate tensile strength level, while C denotes the number of cycles at the intersection of the finite-life region tangent and the asymptote at the fatigue limit level.

The maximum tensile stress $\sigma_{\max}$ was obtained directly from experimental data. The parameters of the model were updated by BUS and PF methods. The PDF curves of the updated model parameters are shown in Figure 6. It can be observed that the marginal posterior PDF functions derived by the BUS and PF methods exhibit no significant differences. The updating effects are notable for parameters σ_{UTS} and b, while the updates for parameters B and C are less pronounced. This is due to the lack of observational data in the regions near the asymptotes of the ultimate tensile strength and the fatigue limit.

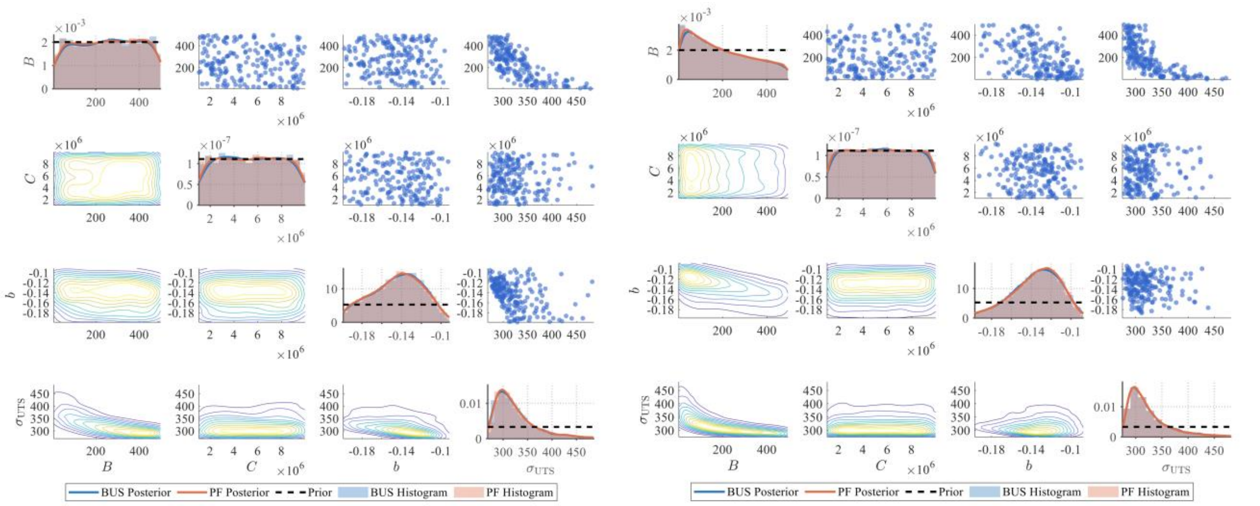

Figure 6. Posterior PDF and Posterior Samples for the K-V Model: (a)Posterior PDF and Posterior Samples in the S direction; (b) Posterior PDF and Posterior Samples in the H direction

3.3. Propagation of Uncertainty in Model Predictions

In Bayesian updating, we infer the posterior distribution of model parameters conditional on observed fatigue life data. By treating fatigue life as the output, parameter uncertainty can be consistently propagated into a predictive distribution for fatigue life, thereby providing a common benchmark for all models. In practical engineering, designers are more concerned with the service life of structural components under given loading conditions and the confidence level of this prediction. The presentation method in this paper directly addresses this question, with the provided life confidence intervals better serving reliability design and risk assessment than traditional single curves.

Model predictions were generated using the updated parameters, with the associated parameter uncertainties propagated to the output to produce 95% confidence intervals for the predictions. A comparison of the predictions from all four models is presented in Figure 7. The confidence intervals of all four models encompass the majority of the experimental data, demonstrating the accuracy of the probabilistic predictions.

It is noteworthy that the prediction confidence intervals of the K-V model exhibit the poorest coverage capability for experimental data. As a stress-based model, the K-V model's complex parameters require joint constraints from both high-cycle and low-cycle fatigue data. The limited low-cycle data available in this study could not effectively update its high-cycle parameters, resulting in high posterior uncertainty for these parameters. This ultimately caused the predicted fatigue life distribution to deviate from the observed data.

Furthermore, comparative observations reveal that at lower fatigue life cycles and under identical strain amplitudes, specimens built in the S direction are more susceptible to fatigue failure, while those in the H direction exhibit superior fatigue performance. This behavior can be attributed to the fact that in S-oriented specimens, the longitudinal axis is parallel to the building direction, causing interlayer interfaces to be perpendicular to the loading direction. This orientation may result in weaker interlayer bonding, facilitating crack propagation along the interfaces and thus reducing fatigue life. In contrast, H-oriented specimens likely possess a more uniform defect distribution, with interlayer interfaces parallel to the loading direction, thereby minimizing the influence of interlayer bonding on fatigue performance and contributing to higher fatigue strength.

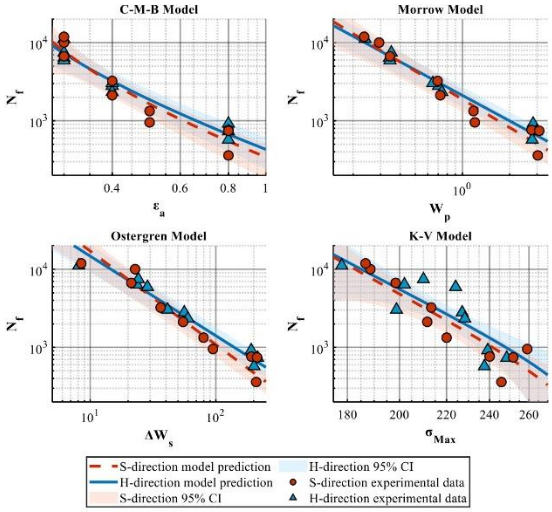

Figure 7. Comparison of Predicted Results from Different Models.

Acknowledgements

This work is supported by the National Natural Science Foundation of China under grant number 12202358 and the Foundation of National Key Laboratory of Strength and Structural Integrity with grant number LSSIKFJJ202402011. The second author is also supported by the National Key R&D Program of China with grant number 2023YFB3407103.

References

Beck, J. L. and Katafygiotis, L. S. Updating models and their uncertainties. I: Bayesian statistical framework. Journal of Engineering Mechanics, 124(4): 455-461, 1998.

Bi, S., Beer, M., Cogan, S., et al. Stochastic model updating with uncertainty quantification: an overview and tutorial. Mechanical Systems and Signal Processing, 204: 110784, 2023.

Blakey-Milner, B., Gradl, P., Snedden, G., et al. Metal additive manufacturing in aerospace: a review. Materials & Design, 209: 110008, 2021.

Coffin, L. F., Jr. A study of the effects of cyclic thermal stresses on a ductile metal. Transactions of the American Society of Mechanical Engineers, 76(6): 931-949, 1954.
DebRoy, T., Wei, H. L., Zuback, J. S., et al. Additive manufacturing of metallic components--process, structure and properties. Progress in materials science, 92: 112-224, 2018.
He, G. Y., Zhao, Y. X., and Yan, C. L. Uncertainty quantification in multiaxial fatigue life prediction using Bayesian neural networks. Engineering Fracture Mechanics, 298: 109961, 2024.
Kohout, J. and Vechet, S. A new function for fatigue curves characterization and its multiple merits. International Journal of Fatigue, 23(2): 175-183, 2001.
Kotadia, H. R., Gibbons, G., Das, A., et al. A review of laser powder bed fusion additive manufacturing of aluminium alloys: microstructure and properties. Additive Manufacturing, 46: 102155, 2021.
Leonetti, D., Maljaars, J., and Snijder, H. H. Uncertainty analysis of constant amplitude fatigue test data employing the six parameters random fatigue limit model. In MATEC Web of Conferences, 165: 10016, 2018.
Liao, D., Zhu, S. P., Gao, J. W., et al. Generalized strain energy density-based fatigue indicator parameter. International Journal of Mechanical Sciences, 254: 108427, 2023.
Liao, X., Wang, Y., Feng, L., et al. Fatigue crack initiation and energy-based life analysis for Q345qD bridge steel at low temperatures. Journal of Constructional Steel Research, 180: 106571, 2021.
Liu, S. and Shin, Y. C. Additive manufacturing of Ti6Al4V alloy: a review. Materials & Design, 164: 107552, 2019.
Manson, S. S. Behavior of materials under conditions of thermal stress. National Advisory Committee for Aeronautics, 1953.
Morrow, J. D. Cyclic plastic strain energy and fatigue of metals. ASTM International, West Conshohocken, PA, 1965.
Oh, B. The exponential law of endurance tests. In Proceedings of the American Society for Testing Materials, 10: 625-630, 1910.
Ostergren, W. J. A damage function and associated failure equations for predicting hold time and frequency effects in elevated temperature, low cycle fatigue. Journal of Testing and Evaluation, 4(5): 327-339, 1976.
Ramirez, B., Banuelos, C., De La Cruz, A., et al. Effects of process parameters and process defects on the flexural fatigue life of Ti-6Al-4V fabricated by laser powder bed fusion. Materials, 17(18): 4548, 2024.
Sanaei, N. and Fatemi, A. Defects in additive manufactured metals and their effect on fatigue performance: a state-of-the-art review. Progress in Materials Science, 117: 100724, 2021.
Sarkar, P. P., De, P. S., Dhua, S. K., et al. Strain energy based low cycle fatigue damage analysis in a plain C-Mn rail steel. Materials Science and Engineering: A, 707: 125-135, 2017.
Song, J., Liang, Z., Wei, P., et al. Sampling-based adaptive Bayesian quadrature for probabilistic model updating. Computer Methods in Applied Mechanics and Engineering, 433: 117467, 2025.
Wang, R., Liu, X., Hu, D., et al. Zone-based reliability analysis on fatigue life of GH720Li turbine disk concerning uncertainty quantification. Aerospace Science and Technology, 70: 300-309, 2017.
Yi, M., Tang, W., Zhu, Y., et al. A holistic review on fatigue properties of additively manufactured metals. Journal of Materials Processing Technology, 118425, 2024.
Zhao, B., Xie, L., Song, J., et al. Prediction of multiaxial fatigue life for complex three - dimensional stress state considering effect of additional hardening. Fatigue & Fracture of Engineering Materials & Structures, 42(11): 2558-2578, 2019.
Zhou, J., Barrett, R. A., and Leen, S. B. Three-dimensional finite element modelling for additive manufacturing of Ti-6Al-4V components: effect of scanning strategies on temperature history and residual stress. Journal of Advanced Joining Processes, 5: 100106, 2022.
Zhu, J. H. A review of topology optimization for additive manufacturing: status and challenges. Chinese Journal of Aeronautics, 34(1): 91-110, 2021.